

Mechanical properties of friction welded 6063 aluminum alloy and austenitic stainless steel

P. Sammaiah · Arjula Suresh · G. R. N. Tagore

Received: 3 December 2009 / Accepted: 10 May 2010 / Published online: 25 May 2010
© Springer Science+Business Media, LLC 2010

Abstract Friction welding of dissimilar metal combination of aluminum alloy and austenitic stainless steel was examined to investigate the effect of welding conditions on mechanical properties of the dissimilar metal combination. The welded joints were produced by varying forge pressure (F_g), friction pressure (F_r), and burn-off length (B). The joints were subjected to mechanical testing methods such as the tension, notch Charpy impact tests. The tensile strength and toughness decrease with an increase in friction pressure. The tensile strength decreases with an increase in burn-off length at a low forge pressure while tensile strength increases with an increase in burn-off length at a high forge pressure. The tensile failure of the welded joint occurred in aluminum alloy just away from interface in the thermo-mechanically affected zone indicates good joint strength at the condition of low friction pressure, high forge pressure, and high burn-off length. The maximum tensile strength was observed with low friction pressure and high forge pressure. The tensile strength of dissimilar joint is approximately equal to tensile strength of 6063 aluminum alloys at the condition of low friction pressure, high forge pressure, and high burn-off length. The tensile and impact failure of joints was examined under scanning electron microscope and failure modes were discussed.

Introduction

It is difficult to join dissimilar metals by fusion welding, such as TIG, MIG, and brazing, due to the different characteristics of each material. Friction welding is the only viable method in this field to overcome the difficulties encountered in the joining of dissimilar materials with a wide variety of thermal and mechanical properties. The advantages of this process among others are no melting, high reproducibility, short production time, and low energy input [1]. The main factor of diffusion bonding is thermal energy, whereas the factors of friction welding are thermal energy by friction and axial force by forging [2].

The welding of aluminum/alloy to steel is of particular interest, since the resulting products join the very different but favorable properties of each component, namely, the high thermal conductivity and low density of Al, and the low thermal conductivity and the high tensile strength of steels [3]. The demand for aluminum alloys/stainless steel joints has therefore increased in many areas including cryogenic applications, spacecraft, high vacuum chambers, and cooking utensils owing to their superior properties. In these structures aluminum has been partially replaced by stainless steel. In this case, it is necessary to join stainless steel to aluminum alloys [4, 5]. The inertia welds of 6061 aluminum to 304L stainless steel dissimilar metal transition joints play a key role in the operation of an accelerator driven, spallation neutron source designed for the production of tritium [6]. A6061-aluminum alloy was joined to a 304 stainless steel by friction welding. The structure of aluminum alloy was refined in the vicinity of the weld interface. However, the Vicker hardness was decreased near the interface since the precipitates were dissolved in the aluminum alloy matrix by the friction heat. The higher friction pressure made the joint strength decrease owing to

P. Sammaiah (✉) · A. Suresh
Department of Mechanical Engineering, S R Engineering
College, Warangal 506371, Andhra Pradesh, India
e-mail: pullasammaiah@gmail.com

G. R. N. Tagore
Department of Mechanical Engineering, National Institute
of Technology, Warangal 506004, Andhra Pradesh, India

the excess formation of brittle intermetallic (IM) compounds at the weld interface [7]. Friction welding of 6061 aluminum alloy and steel was conducted. Sound welds were produced in all A6061/steel combinations and tensile fracture occurred in the thermal-softened A6061 area. Joint strength depends on the width of this softened A6061 area [8]. In case of A6061/S45C joint, the joint strength increases with an increase in forging pressure, and iron-aluminum alloy is observed at the weld interface. The effect of forge pressure on microstructure at the weld interface depends on the deformation property of each aluminum alloy at an elevated temperature [8]. The dissimilar material combination of commercially pure aluminum and austenitic stainless steel is difficult to weld on account of the formation of brittle IM phases and the wide difference in physical and mechanical properties. Friction welding, by virtue of its low and controlled energy input and rapid thermal cycle, offers a viable solution to these problems [9].

As the thermal conductivity of aluminum is more than austenitic stainless steel, most of the heat supplied at the interface is conducted toward aluminum side resulting in thermal softening in greater width. Due to recrystallization, the tensile strength is shortly reduced while the ductility is increased. At this juncture, it is understood that a proper relation can be seen between the amount of cold work and the grain size. This is to say that the fineness of the grain size will be improved when there is an increase in the cold work. Hence, higher forging pressures decrease the grain size [10]. The higher the degree of cold work, the higher the rate of recrystallization that results in the higher nucleation rate and finer grains [11]. In case of austenitic stainless steel and ferritic steel friction-welded joints [12], austenitic stainless steel does not undergo extensive deformation while ferritic stainless steel specimen undergoes extensive deformation. The same phenomenon has been observed during friction welding of dissimilar welds, namely aluminum to copper, titanium to steel, aluminum to steel, etc. [13–16]. In this study, the experiments were carried out to investigate the effect of welding parameters on mechanical and metallurgical properties of friction welded 6063 aluminum alloy and AISI 304 austenitic stainless steel.

Experimental

Materials

Materials used in this study were 6063 aluminum alloy and commercial AISI 304 austenitic stainless steel couple. The compositions of the parent metals (PMs) are shown in Table 1. Mechanical and thermal properties of PMs are

Table 1 Chemical composition of materials

| Alloying element | Cu | Mg | Si | Fe | Mn | Zn | Ti | Cr |
|-------------------------------------|------|---------|---------|------|------|-----|-----|------|
| 6063 aluminum alloy | | | | | | | | |
| Composition (wt%) | 0.1 | 0.4–0.9 | 0.3–0.7 | 0.6 | 0.3 | 0.2 | 0.2 | 0.1 |
| Alloying element | | | | | | | | |
| C | Si | Mn | Cr | S | P | Ni | Fe | |
| AISI 340 austenitic stainless steel | | | | | | | | |
| Composition (wt%) | 0.06 | 0.32 | 1.38 | 18.4 | 0.28 | 0.4 | 8.7 | Bal. |

Table 2 Mechanical and thermal properties of materials

| Material | Tensile strength (MPa) | Thermal conductivity (W m/K) | Coefficient of thermal expansion (K) |
|---------------|------------------------|------------------------------|--------------------------------------|
| 6063 Al alloy | 215 | 180 | 23×10^{-6} |
| AISI 304 | 515 | 16.2 | 17.2×10^{-6} |

shown in Table 2. Austenitic stainless steel rod of 75 mm and 6063 aluminum alloy rod of 100 mm lengths with equal diameter of 16 mm were used in this experimental work.

Friction welding

Welding was performed on a continuous drive friction welding machine at a speed of 1,500 rpm in a variable speed machine of 10 kN capacity. The aluminum alloy rod is fixed in a rotating member while stainless steel rod is fixed in a stationary member. The welding parameters used in this study are shown in Table 3. In the continuous drive friction welding process a stationary member (austenitic stainless steel rod) is pressed against a rotating member (aluminum alloy rod) with an axial pressure. The relative motion generates frictional heat, which causes the material to soften and plastically deform. After a preset displacement has occurred, the machine is halted, and the pressure is increased to generate a high quality solid-state weld. During welding the primary parameters (friction pressure, forge pressure, burn-off length, and rotational speed) were continuously monitored and recorded. Few more trials have been carried out with different parameters in order to get defect free welds. The main parameters employed are friction pressure, forge pressure, and burn-off length

Table 3 Welding parameters used in the study

| Parameters | |
|-------------------------|------------|
| Friction pressure (MPa) | 24, 73, 98 |
| Forge pressure (MPa) | 98, 146 |
| Burn-off length (mm) | 1, 2, 3 |

(length loss during friction/forge stage). Trial welds were produced by varying one parameter and keeping other parameters constant to find the limits.

Mechanical testing

The mechanical tests consist of tensile test, Charpy “V” notch impact test and Vickers micro hardness testing. Tensile samples of welded joints were prepared according to ASTM-E8 standard. The tensile tests were carried out in an Instron 1185 universal testing machine to record the tensile strength at cross head speed of 0.5 mm/min. The joint efficiency is measured in terms of the tensile strength of welded metal divided by tensile strength of weaker metal of dissimilar metals [4].

The impact resistance of a material is the ability of a material to resist breaking under a shock loading. The impact strength reflects the toughness of the material since the impact energy is dissipated by elastic or plastic

deformation of the material. The impact properties (at room temperature) were measured by Charpy “V” notch impact test. The V-notch is prepared at the interface of friction-welded sample according to Charpy test dimensions using milling machine. The Charpy impact test specimen is shown in Fig. 1.

The micro hardness of samples was measured using MMT-3 micro hardness tester under a load of 100 g. The readings were taken on aluminum alloy and austenitic stainless steel sides across the weld interface.

Metallography

Low magnification stereomicroscope of Leitz make was employed for observing the microstructure of welded joint. Microstructural features and grain deformation were observed in a Leo Scanning electron microscope. Fractography of fracture of welds in tensile and impact tests was carried out under a Leo scanning electron microscope.

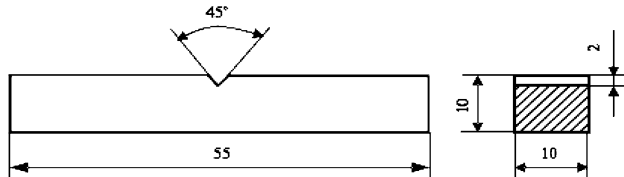


Fig. 1 Impact test sample of friction welded dissimilar metals

Results and discussion

Appearance and microstructure of welded joints

The appearance of friction-welded joints of 6063 aluminum alloy and austenitic stainless steel is shown in Fig. 2.

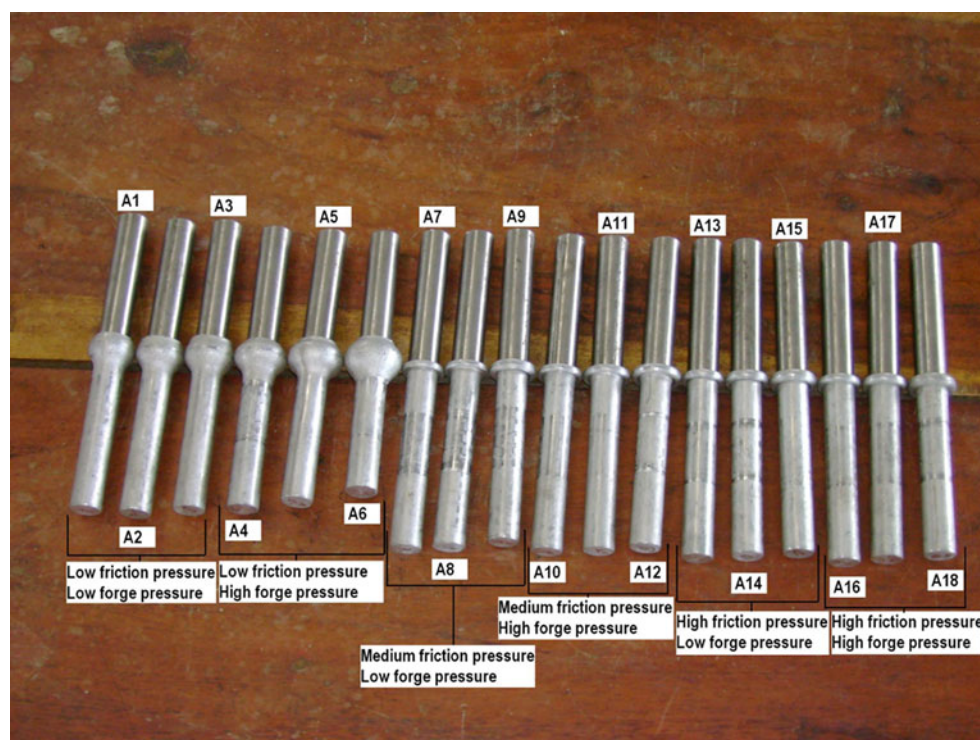


Fig. 2 Appearance of friction-welded joints of 6063 aluminum alloy and 304 stainless steel

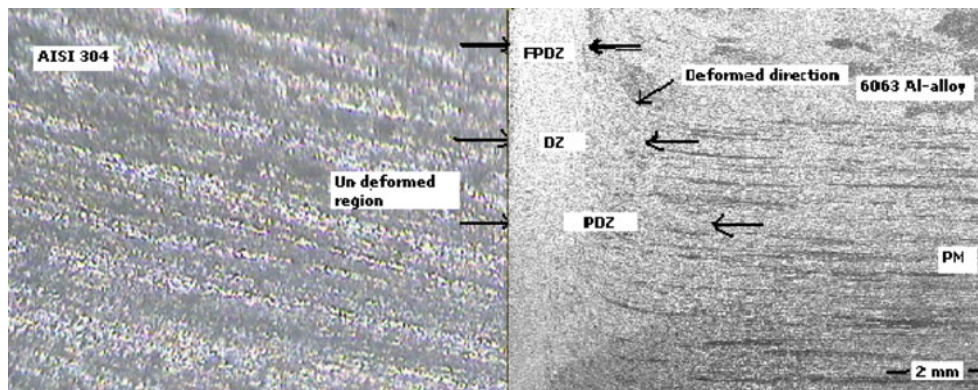


Fig. 3 The microstructure at welding interface and representation of interface reactions

The joint exhibits higher flash with increase in burn-off and forge pressure with constant friction pressure. The flash was observed to be from aluminum alloy side and austenitic stainless steel did not participate in the flash formation suggesting deformation is mainly limited to aluminum alloy side. Microstructural evaluation of friction-welded joints revealed four distinct zones across the specimens which were identified as PM, partial deformed zone (PDZ), deformed zone (DZ) and transformed and recrystallized fully plasticized deformed zone (FPDZ) (see Fig. 3). The different thermal and physical properties of the materials to be welded in dissimilar metal welding (heat capacity, thermal conductivity, relation between hardness and temperature) generally results asymmetrical deformation. Austenitic stainless steel has much lower thermal conductivity and greater hardness at higher temperatures compared to aluminum alloy. For this reason austenitic stainless steel does not undergo extensive deformation while aluminum alloy specimen undergoes extensive deformation (Fig. 3). The same phenomenon has been reported during friction welding of dissimilar welds, namely aluminum to copper, titanium to steel, aluminum to steel, etc. [13–16]. The formation of upset collar (flash) on

the austenitic stainless steel side only is due to low strength of aluminum alloy. This shows that only aluminum alloy takes part in upset collar formation is substantiated by the shortening of the aluminum alloy rod only. The width of the deformation zone increases with increase in burn-off length [13]. The deformation zone would be wider at low burn-off than at high burn-off could be attributed to lower heat content and high flow stress of the region at low burn-off than when the burn-off is high that aids in the spread of heat resulting in increased heat content and consequent lowering of flow stress in this region [13]. The central region of weld consists of fine grains, while the peripheral region consists of coarse grains (Fig. 4). The fine grain size at the central region is due to dynamic recrystallization. The temperature of the peripheral region would be higher [17] and therefore exhibits coarse grain size.

Mechanical properties

The mechanical and thermo-physical properties of dissimilar substrates will have a major influence on the properties of the dissimilar joints because the temperature attained by each substrate markedly depends on the

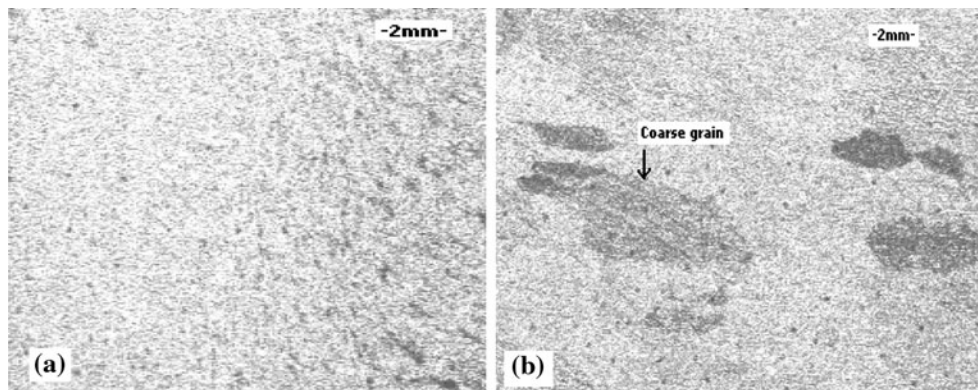


Fig. 4 Microstructure showing **a** fine grains at center and **b** coarse grains at periphery of the weld

Table 4 Tensile strength and toughness of friction-welded joints produced under different welding conditions

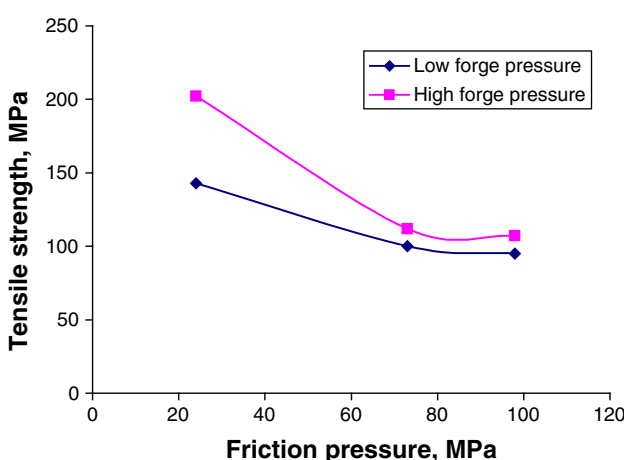
| S. No. | Welding parameters | | | Mechanical properties | | |
|--------|--------------------|-------------|----------|------------------------|---------------|------------------|
| | F_r (MPa) | F_g (MPa) | B (mm) | Tensile strength (MPa) | Toughness (J) | Joint efficiency |
| 1 | 24 | 98 | 1 | 150 | 34 | 70 |
| 2 | 24 | 98 | 2 | 143 | 35 | 66 |
| 3 | 24 | 98 | 3 | 141 | 35 | 66 |
| 4 | 24 | 146 | 1 | 146 | 66 | 68 |
| 5 | 24 | 146 | 2 | 151 | 66 | 70 |
| 6 | 24 | 146 | 3 | 202 | 68 | 94 |
| 7 | 73 | 98 | 1 | 108 | 25 | 50 |
| 8 | 73 | 98 | 2 | 99 | 40 | 46 |
| 9 | 73 | 98 | 3 | 115 | 31 | 53 |
| 10 | 73 | 146 | 1 | 119 | 26 | 55 |
| 11 | 73 | 146 | 2 | 134 | 36 | 62 |
| 12 | 73 | 146 | 3 | 111 | 28 | 52 |
| 13 | 98 | 98 | 1 | 124 | 26 | 57 |
| 14 | 98 | 98 | 2 | 94 | 25 | 44 |
| 15 | 98 | 98 | 3 | 102 | 25 | 47 |
| 16 | 98 | 146 | 1 | 116 | 25 | 54 |
| 17 | 98 | 146 | 2 | 96 | 26 | 44 |
| 18 | 98 | 146 | 3 | 106 | 34 | 50 |

thermo-physical properties of the two substrates and on the joining parameters selected. Consequently, the flow stress–temperature relations for each substrate will have an important influence on the joint properties produced during friction welding [12].

The result of the tensile strength and impact toughness measurements for the Al alloy/stainless steel friction-welded pair are shown in Table 4. Figure 5 shows the tensile strength dependence on friction pressure of Al alloy/stainless steel friction-welded joint. The tensile strength

decreases with an increase in friction pressure at both the low forge pressure and high forge pressure. This is due to high heat generation that leads to coarse grain structure. The periphery of the friction-welded sample shows coarse grain structure (Fig. 4) due to high heat generation (maximum friction). It is observed that at high temperatures flow stresses are decreased whereas grain size becomes coarser. In contrast, at relatively low temperatures, finer grain sizes are obtained while flow stresses are increased. The center of the sample shows fine grain structure due to low heat and high degree of cold working. The higher is the degree of cold work, the higher the nucleation rate and the finer the grains. The tensile strength is higher with the higher degree of cold working. The fine microstructural features at high forge pressures can be attributed to the higher strain energy while the coarse microstructures are due to prolonged retention time at high temperature that resulted in grain coarsening. The coarse grains are caused by higher temperature due to high friction pressure distribution at periphery. The deformation rate depends on heat developed at the interface during friction welding, which depends on friction pressure and burn-off length. The tensile strength decreases with an increase in burn-off length at low forge pressure while tensile strength increases with an increase in burn-off length at high forge pressure as it can be seen in Fig. 6.

The tensile strength is higher at low friction pressure and high forge pressure due to more plastic deformation and

**Fig. 5** Variation of tensile strength with friction pressure (burn-off length 3 mm)

higher flash at interface (i.e., Joint efficiency = 94%). The flash developed at interface due to forge pressure and it increases with an increase in forge pressure and takes place

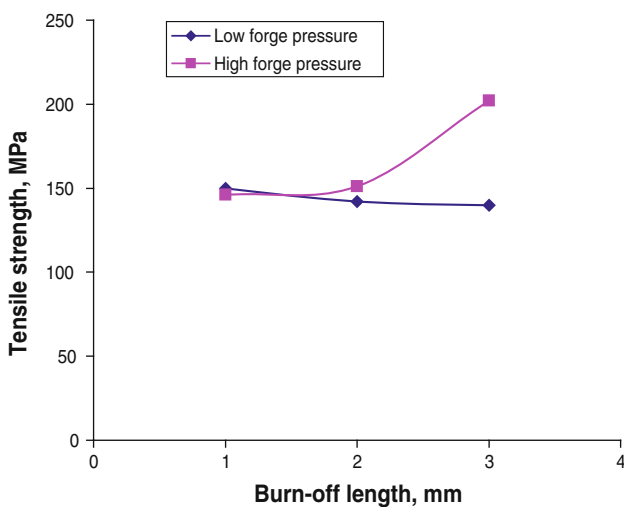


Fig. 6 Variation of tensile strength with the burn-off length (friction pressure 24 MPa)

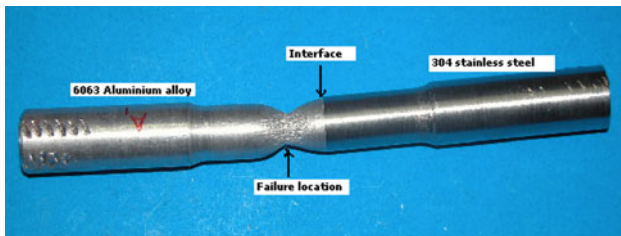


Fig. 7 Tensile failure of friction-welded joint (24-146-3) away from the weld interface

in aluminum alloy side only. Figure 7 shows the tensile failure of welded joint produced under low friction pressure and high forge pressures. It can be seen that the failure is in the aluminum side away from weld line indicating the strong weld interface. Micrograph in Fig. 8 confirms the ductile mode of tensile failure.

The tensile strength is lower at high friction pressure and low forge pressure that resulted in poor deformation and lower flash at the interface (i.e., Joint efficiency = 70%). The higher friction pressure decreases the strength due to the excess formation of brittle IM compounds at the weld interface [13]. It was observed that the tensile strength decreases with increasing of IM layer thickness. Figure 9 shows the failure of the welded joint at the weld interface indicating poor strength of the joint. The formation of IM phase can be seen in micrographs shown in Fig. 10. The micrograph indicates the brittle fracture of the joint.

The impact strength/toughness increases with an increase in burn-off length for both the low forge and high forge pressures (Fig. 11). This is resulting due to equiaxed

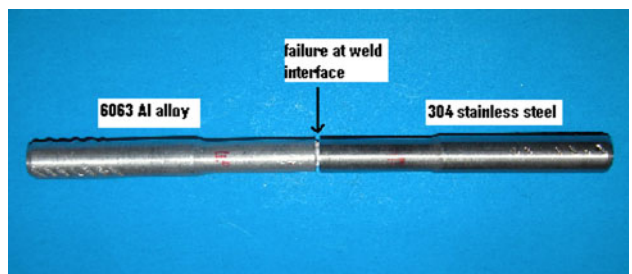


Fig. 9 Tensile failure of friction-welded joint (98-98-3) at the weld interface

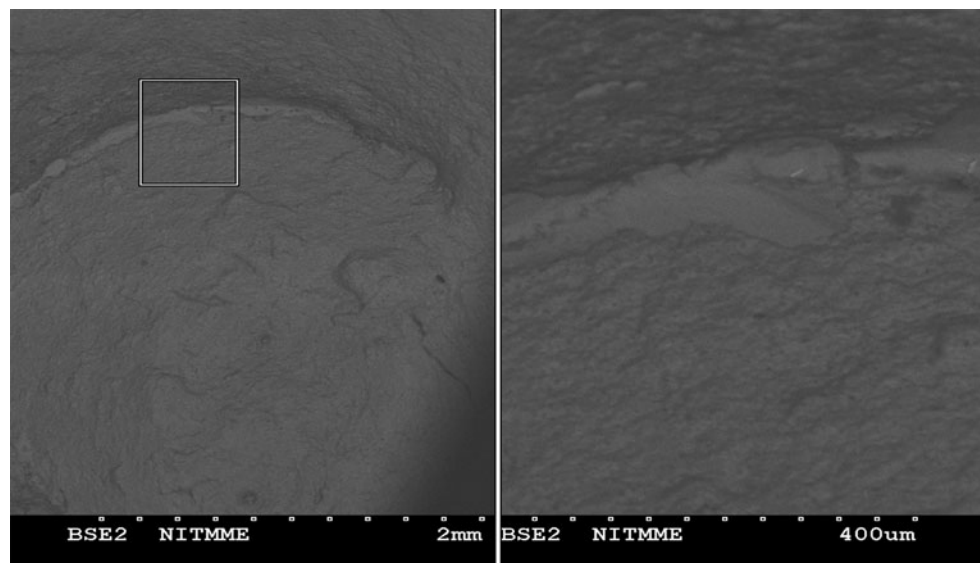


Fig. 8 SEM micrograph showing ductile failure in the aluminum alloy side of welded joint (24-146-3)

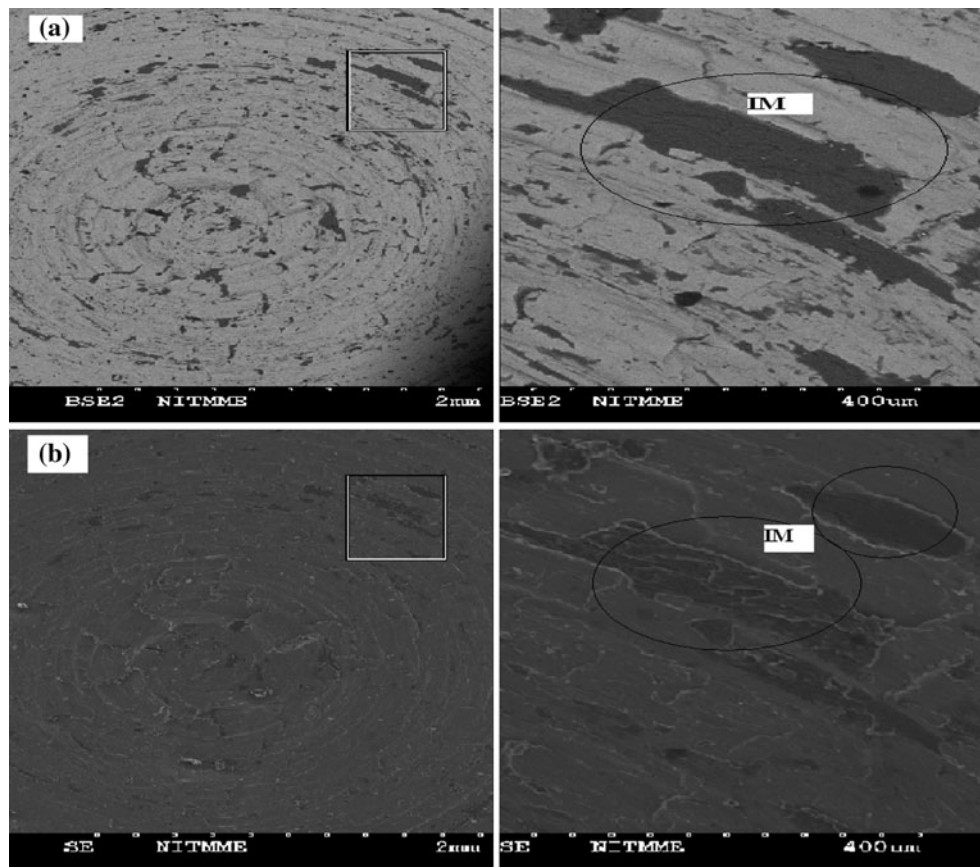


Fig. 10 SEM micrographs of fractured surface of tensile specimen of welded joint at 98-98-3: **a** aluminum alloy side and **b** austenitic stainless steel side

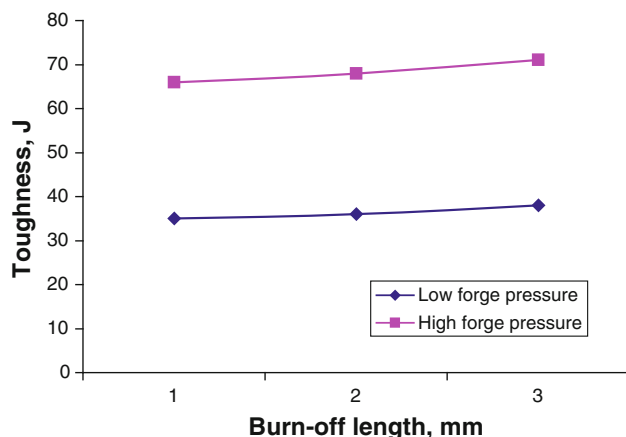


Fig. 11 Variation of toughness with burn-off length (friction pressure 24 MPa)

fine grain formation with higher degree of working at the interface. The higher the degree of cold work then the higher the rate of recrystallization which gives the higher nucleation rate and finer grains. Figure 12 shows variation

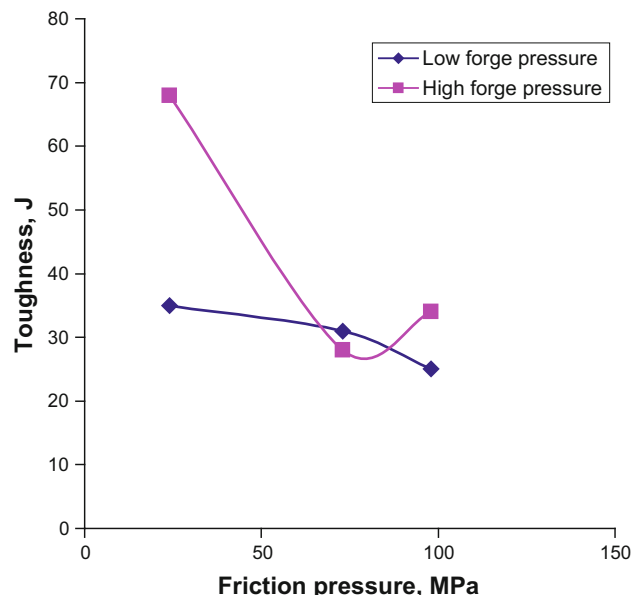


Fig. 12 Variation of toughness with friction pressure (burn-off length 3 mm)

of impact strength/toughness with friction pressure. The toughness decreases with increasing friction pressure. This is due to high heat generation, which results in coarse grain structure and IM formation. The fracture shows brittle failure due to IMs at interface as shown in Fig. 13. Toughness is higher with the high forge due to higher deformation and failure occurs little bit away from the interface is evidenced by failure away from the interface and fracture shows ductile failure (Fig. 14). This supports the fact that joint has good interface, which is formed with good toughness. Micrograph in Fig. 15 confirms the ductile mode with micro voids of impact specimen (24-146-3). The tensile strength of welded joint (24-146-3) is approximately equal to the tensile strength of weaker material (aluminum alloy) as shown in Table 5. However, the failure in aluminum side is due to thermal softening in wider heat affected zone. Sound weld is produced in weld combination (24-146-3) and tensile fracture is occurred in the thermal-softened 6063 area.

Figure 16 shows the typical distribution of hardness across the weld line. This reveals that hardness is higher on austenitic stainless steel side of the interface. The micro hardness is improved at the interface with welding parameters. The micro hardness is higher at interface with the condition of low friction, high forge, and high burn-off length (24-146-3). An increase in hardness is observed in austenitic stainless steel due to strain hardening in the DZ (Fig. 16). The micro hardness trend suggests that low friction pressures and high forge pressures lead to high hardness. This is due to lesser heat input available at the center resulting high degree of working. This situation leads to similar conditions to cold working where the hardness increases commensurate with the degree of cold working. This high hardness due to heavy cold working is a result of high-density dislocations during plastic deformation. The hardness increases continuously with an increase in deformation rate because the dislocation distribution is attributed to the presence of fine precipitate

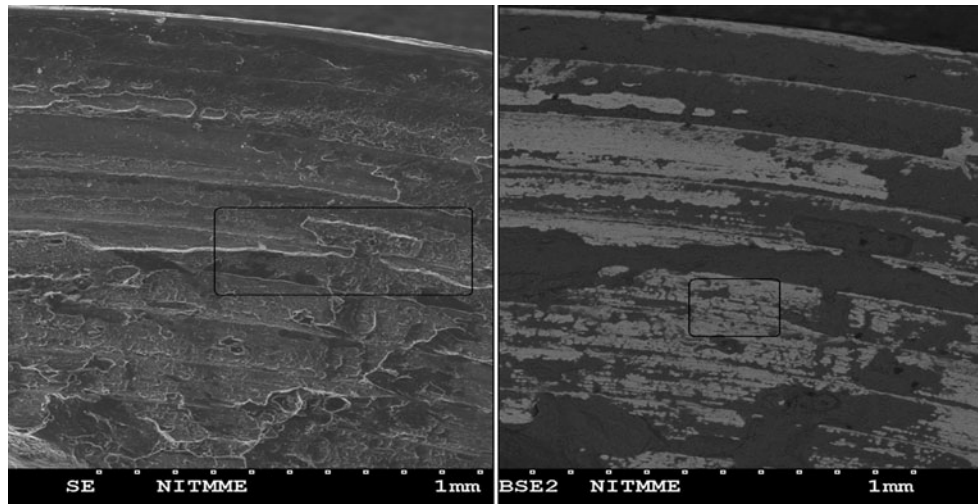


Fig. 13 SEM micrograph of fractured surface of impact test specimen of aluminum alloy and austenitic stainless steel (98-98-3)

Fig. 14 Appearance of fracture surface of (ductile mode) of the impact test specimen (24-146-3)



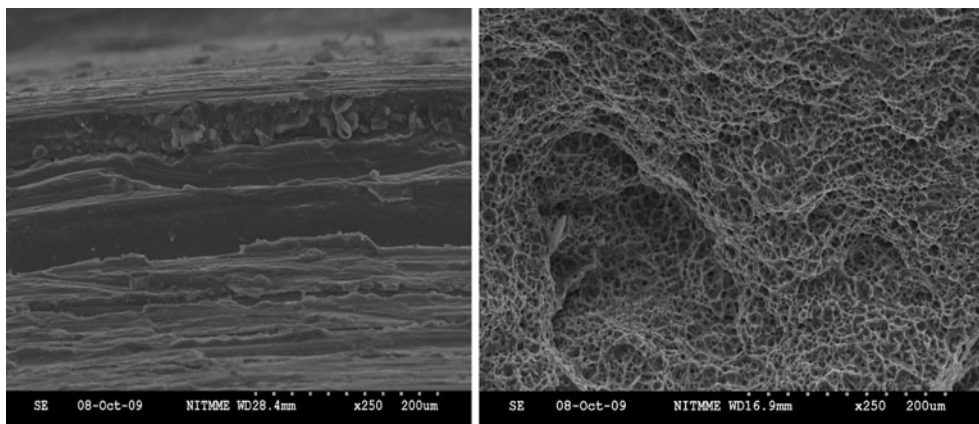


Fig. 15 SEM micrograph of fractured surface of impact specimen of welded joint (aluminum alloy side)

Table 5 Comparison of tensile strength and impact toughness for parent metals and welded joint (24-146-3)

| Material | Tensile strength (MPa) | Toughness (J) |
|-------------------------------------|------------------------|---------------|
| AISI 304 austenitic stainless steel | 580 | 200 |
| 6063 aluminum alloy | 215 | 25 |
| Welds of dissimilar material | 202 | 67 |

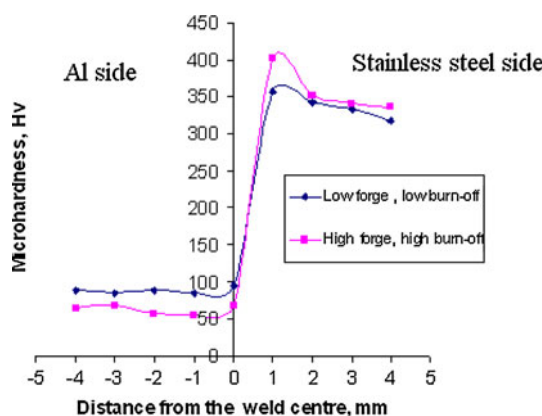


Fig. 16 Distribution of micro hardness across the weld interface

particles, which interact with the dislocation and therefore prevent recovery [18].

Conclusions

The present study was conducted to investigate the metallurgical and mechanical properties of friction welds of 6063 aluminum alloy and AISI 304 austenitic stainless steel couple. The effects of welding parameters on metallurgical and mechanical properties of friction-welded joints were investigated, and the correlation between the

microstructure and the joint strength was discussed. The following conclusions are drawn from the present study:

1. Low friction pressure, high forge pressure, and high burn-off length results higher deformation and higher flash. The higher deformation results in higher tensile strength and good toughness.
2. The microstructure shows fine grains at center and coarse grains at periphery with the condition of low friction, high forge and high burn-off length.
3. The tensile strength and toughness decrease with an increase in friction pressure. The micro hardness at interface is higher at the condition of high forge and high burn-off length. The tensile strength of friction-welded joint is approximately equal to tensile strength of aluminum alloy.
4. Higher forge pressure combinations exhibit fine grain size and increased friction pressure aids in grain coarsening.
5. The toughness of dissimilar metal welds are better than aluminum alloy PM at low friction pressures while toughness is lower than aluminum alloy at high friction pressures.
6. The scanning electron micrograph shows the ductile fracture occurred at low friction and high forge pressures in aluminum alloy whereas brittle fracture occurred at high friction and low forge pressures in the interface due to the formation of IM compounds.

Acknowledgments The authors express their gratitude to Defence Research and Development Organization for the microstructure analysis to carry out this programme. The authors are thankful to Dr. G. Madhusudhan Reddy, DMRL for his continued encouragement. The author also thanks to Prof. K. Prasada Rao (IIT M) for the support to conduct the experimental work. One of the authors (P. Sammaiah) is thankful to the Principal and the management of S.R. Engineering College, Warangal for their continued support during this work.

References

1. Ruge J, Thomas K, Eckel C, Sundaresan S (1986) Weld J 65:28
2. Kim HJ, Kang JY, Shin YE, Kim DS (1998) Welding handbook. Korea Welding Society, Seoul, p 659
3. Yilmaz M (1993) Investigation of welding area in the friction welding of tool steels. PhD thesis, Yildiz Technical University, Istanbul, Turkey
4. Fukumoto S, Tsubakino H, Okita K, Aritoshi M, Tomita T (1998) Mater Sci Technol 14:333
5. Fukumoto S, Tsubakino H, Okita K, Aritoshi M, Tomita T (1999) Mater Sci Technol 15:1080
6. Dunn KA, Tosten MH, Louthan MR, Birt ML (1999) In: 32nd international metallographic society annual convention, OH, USA, 31 Oct–3 Nov, 1999
7. Fukumoto S, Ohashi M, Tsubakino H, Okita K, Aritoshi M, Tomita T, Goto K (1998) J Jpn Inst Light Met 48(1):36
8. Ochi H, Ogawa K, Yamamoto Y, Suga Y (1996) J Soc Mater Sci 45(4):459
9. Sundaresan S, Murti KGK (1993) Join Mater 5(2):66
10. Yokoyama T, Yamaguchi M (1999) J Jpn Inst Light Met 49(9/11):535
11. Olorunniwo OE, Atanda PO, Akinluwade KJ (2009) J Miner Mater Charact Eng 8(1):1
12. Satyanarayana VV, Madhusudhan Reddy G, Mohandas T (2005) J Mater Process Technol 160:128
13. Yilmaz M, Col M, Acet M (2003) Mater Charact 49:421
14. Kim S-Y, Jung S-B, Shur C-C (2003) J Mater Sci 38:1281. doi: [10.1023/A:1022890611264](https://doi.org/10.1023/A:1022890611264)
15. Bekir SY, Ahmet ZS, Nafiz K, Ahmed Z (1995) J Mater Process Technol 49:431
16. Jessop TJ (1995) Friction welding of dissimilar metal combinations-aluminum and stainless steel. Weld Institute Research Report, November 1995, pp 73–75
17. Fukumoto S, Tsubakino H, Aritoshi M, Tomita T, Okita K (2002) Mater Sci Technol 18:219
18. Deschamps A, Brechet Y, Guoyat P (1999) In: Proceedings of the seventh seminar of the international federation of heat treatment and surface engineering, Hungary, pp 1–10